


Effect of compression precracking on near threshold region for AISI 4340 steels considering compliance measurements

Salim Çalışkan , Rıza Gürbüz 

Middle East Technical University, Ankara, Turkey

caliskan.salim@metu.edu.tr

Abstract. Determining long crack threshold as a design criterion is not a new research topic; however, some anomalies because of different test methods in literature keep it vogueish. Inaccurate estimations may result in considerable variation on corresponding endurance stress for components with small crack size. Accepted approach compared to traditional methods is to perform compression-compression precracking before crack growth tests by eliminating history effects and accurately estimating long crack threshold value. Load history effects may result from specimen configuration and test procedure applied. The scale of yielding during precracking cannot be underestimated and these residual stresses have an effect on crack growth rates, even if limited by stress relief in the plastic region. Naturally formed precrack will propagate until diminishing size of the corresponding tensile zone responsible for crack growth. Compression-compression precracking under constant amplitude loading is performed to form non-propagation crack. The advantage of compression precracking is to provide a fully open crack that eliminates possible closure effects. In the scope of this paper, different stress ratios will be tested and the effect of compression precracking on near threshold will be investigated. To present reliable and accurate crack measurement that affects long threshold directly, compliance curves will be also introduced with this article.

Keywords: Steel, Fatigue, Compliance, Crack growth, Threshold

Acknowledgments. Authors acknowledge Turkish Aerospace Inc.

Citation: Çalışkan S, Gürbüz R. Effect of compression precracking on near threshold region for AISI 4340 steels considering compliance measurements. *Materials Physics and Mechanics*. 2023;51(1): 151-167. DOI: 10.18149/MPM.5112023_13.

Introduction

Damage tolerant design approach is used for components having high cycles of operation life such as transmission parts and service life and inspection intervals are specified based on fatigue crack growth data [1]. Fatigue crack propagation behavior is caused by intrinsic and extrinsic mechanisms. Intrinsic mechanism can be controlled by monotonic and cyclic strains ahead of crack tip. Brittle materials exhibit monotonic loading fracture; on the other hand, ductile ones show cyclic deformation because of crack blunting and re-sharpening in the vicinity of steady state crack propagation. Cyclic plastic deformation is the reason for fatigue crack growth with below fracture toughness loading over ductile materials. Generation of residual stresses because of plastic deformation after unloading results in change in local stress ratio and fatigue crack growth behavior is severely affected as if applied additional loading [2]. Steels exhibit strain hardening under deformation and expected stress redistribution is to be less and results as smaller plastic zone size ahead of crack tip [3]. Fatigue cracks grow through slip planes with

maximum resolved shear stress and shear stress changes grain to grain, therefore crack path has a rough surface.

Historically, compression precracking is proposed for materials having low fracture toughness and possible failure occurs under tensile precracking conditions. Compression precracking was proposed by Hubbard to eliminate possible load history effects and generate accurate crack growth rates around near threshold [4]. After compression precracking, non-propagating crack needs to advance at least three monotonic compressive zone sizes to reach steady state crack growth conditions. Compression precracking followed by constant amplitude loading is considered as favorable procedure for analyzing threshold behavior of long cracks at low stress amplitudes.

Pearson observed propagation of small cracks below long crack threshold stress intensities defined by test standards [5]. Then, Newman assessed different behavior of small and long cracks around near threshold on remote crack closure effects that are effective on long cracks under constant amplitude loading [6]. Small cracks below certain length grow faster than long ones because of absence of crack closure. Elber identified crack closure concept under alternating loading that affects residual stress distribution and plastic wake around crack flanks, and this phenomenon is known as load history effects on crack propagation [7]. James et al. studied possible load history effects caused by compression precracking as tensile residual stress that increased threshold value. Load history effects can be due to specimen configuration and applied test procedure. Scale of yielding during precracking cannot be underestimated and has an effect on crack growth rates, even though those residual stresses are limited in plastic zone due to stress relief [8]. Fanning around near threshold is caused by load history and environmental effects resulting in remote closure. Maierhofer et al. described crack growth rate model for small cracks having small scale, yielding by building up crack closure effects and Modified NASGRO equation. Each closure mechanism occurs entirely after certain crack extension. Plasticity induced crack closure increases because of increasing plastic zone size until definite crack size and becomes constant [9]. Some equations were introduced to correlate crack growth rate with ΔK (stress intensity factor) for all three regions of da/dN (a : crack size and N : number of fatigue cycles) curve. Steady state and unstable crack growth regions are generally fitted well, but problematic region is around near threshold, especially for lower stress ratios [10].

Fatigue limit can be expressed as resistance of material in terms of propagation of nucleated cracks and corresponding threshold stress for fatigue limit needs to be overcome microstructural barriers for growth process. Therefore, fatigue limit is directly correlated with microstructure properties like grain dimensions at onset of fatigue initiation and initial growth phase can also be called as microstructural threshold. By controlling microstructure through heat treatment enables to have superior fatigue properties of material via excellent mechanical properties. Microstructurally short cracks (on the order of grain size) endure crack propagation because of microstructural barrier resistance and arrest results in preserving fatigue limit unchanged until certain size. Those cracks generally nucleate on surface, and threshold stress is called smooth or plain specimen fatigue limit. However, long cracks have sufficient driving force for growth and fatigue limit decreases by increasing crack size [11]. Applied ΔK needs to be higher than threshold value that is related with crack closure phenomenon for growth process for long cracks. Physically small cracks are between microstructural small cracks and long cracks and crack closure starts to become effective, even though they are also sensitive to microstructural changes. This range can be considered as 50 μm and 0.5 mm crack size for low carbon steels [12]. Below 50 μm ; microstructural shot crack is prevailing, and fatigue limit not affected by microstructural barriers. However, fatigue limit starts to decrease parabolically increasing crack size until reaching long crack size region. Then; fatigue limit has a linear relation with increasing crack size because of losing crack closure effects that is responsible

asymptotically decrease for physically short cracks. Number of cycles in terms of fatigue life are spent during propagation phase for most of the short cracks.

Small crack growth is affected by microstructural changes, large scale yielding at crack tip and crack closure as driving force for propagation. In pearlite phase, crack propagation rate decreases because of thin ferrite lamellar on the microstructure; however, cementite part is responsible for rapid propagation Linear Elastic Fracture Mechanics (LEFM). In microstructure containing ferrite and bainite phase; cracks start on ferrite phase and propagate through ferrite across retained austenitic regions [13]. Fatigue growth for small cracks needs to have higher internal and applied stress because of less closure effects. By increasing crack length, internal stresses due to dislocation pile-up to sustain crack growth decrease, which is inversely proportional with R curve change. Specimen with short cracks requires higher stress amplitude and large number of cycles to develop fatigue damage near crack tip, necessary growth of crack [14]. Short cracks grow very slowly by in high propagation rates compared to long cracks. Threshold of stress intensity range for small cracks increases until asymptote to long crack threshold value by increasing crack length and variation of this phenomenon is called R-curve or resistance curve to fatigue crack propagation. This curve serviceably helps to evaluate fatigue limit of materials having small size defects [15]. SN curves can be considered as a function of small crack initiation in classical safe life design approach [16].

Source of internal stresses is stress concentration regions such as notch, hole, microstructural defects etc. and internal stress asymptotically decreases by distance move away. However, applied stress increases by increasing crack length and there exist competitions in terms of total stress. If applied stress is less than ΔK_{th} (threshold stress intensity factor) and K_{max} (maximum stress intensity factor), crack is arrested since total stress is insufficient for propagation. Elimination of internal stress is attributed to fatigue crack growth behavior of long cracks. Local stress ratio will be higher at crack tip than remote load ratio because of existence of internal stresses. Essentially, equal driving forces exist for fatigue crack growth behavior between short and long cracks in case of all the forces included. Compressive residual stresses result in extra stiff characteristic to material and higher driving forces require for crack growth. Therefore, compressive residual stresses enhance crack closure. Change in grain boundary orientation due to strain concentration may be the reason for arresting of small cracks [17].

Short crack behavior exhibits unlike than long crack in terms of difference in crack closure, microstructural sensitivity and relative plastic zone size based on crack length. It is known that short cracks grow at higher propagation rates. Basically, small cracks can be classified into four groups. Microstructural small crack: it is less than grain size. Mechanically small crack: it is less than plastic zone size. Physically small crack: it is less than a unity, so crack closure is fully formed (considered as 1 mm). Chemically small crack: it depends on crack tip environment and may be up to 10 mm in size. Short crack growth rate is faster than long ones, and even they can propagate below long crack threshold region. Long fatigue life can be reached by understanding the near threshold concept and choosing design loads around threshold value. Damage tolerant design allowed to use structures with crack with known propagation rates and specifying inspection interval for remedy. Previously, safe life approach focused only operation lifetime of a component and replacing part after retirement without inspected whether existence of a crack or not. Safe life design is still in use for primary structures based on defining fatigue limit; however, damage tolerant design approach become popular because of extended life of components. Therefore, crack propagation rates become a significant issue during design phase. On material selection phase, it is desired to be high fatigue crack growth resistance with high threshold value fulfilled with soft material that is in contrast with fatigue limit. Therefore, optimum one is chosen for design material by providing less crack growth rate and high fatigue limit [18]. Fatigue crack propagation behavior for small cracks has different curve shape compared to long ones. Many analytical models are introduced to predict

crack growth rate. It is known that short cracks will extend their crack size even though applied stress is below the corresponding long crack threshold value. Therefore, residual life of a component is remarkably affected with altering threshold value. Change in $1 \text{ MPa}\sqrt{\text{m}}$ on threshold value results in about 18% change in residual characteristics of a component [19].

Experimental Procedure

Crack growth test specimens were manufactured from AISI 4340 steel with a chemical composition of .38% C, .65% Mn, .7% Cr, 1.65% Ni, .2% Mo, .025% P and S, bal. Fe (in wt%) to discover crack propagation behavior of the steel having high toughness and fatigue performance that makes it good candidate as an aerospace grade material. Crack growth tests were carried out by Single Edge Bending (SEB) specimens. In total, four specimens were used for crack growth tests, and they were extracted in rolling direction. After the material was out of stock, heat treatment was applied per AMS 2759-1D [20]. Accordingly, the rectangular bar was initially normalized at $900 \text{ }^\circ\text{C}$ for 90 minutes then air cooled, austenitized $816 \text{ }^\circ\text{C}$ for 60 minutes followed by quickly oil quenched and finally tempered $600 \text{ }^\circ\text{C}$ for 3 hours. After heat treatment, bainite and ferrite phases are available in microstructures as shown in Fig. 1. Machining parameters were 450 m/min cutting speed, 0.25 rev/min coarse gain and 0.1 rev/min fine gain. The dimensions of specimens were 110 mm in length, 24 mm width and 12 mm thickness by ensuring plain strain condition specified on ASTM E647 [21]. Also, notch section with 8 mm width was produced by Electro Discharge Machining (EDM) method to provide high accuracy in terms of positioning. Mechanical properties can be summarized as 1080 MPa tensile strength and 29 HRC hardness.

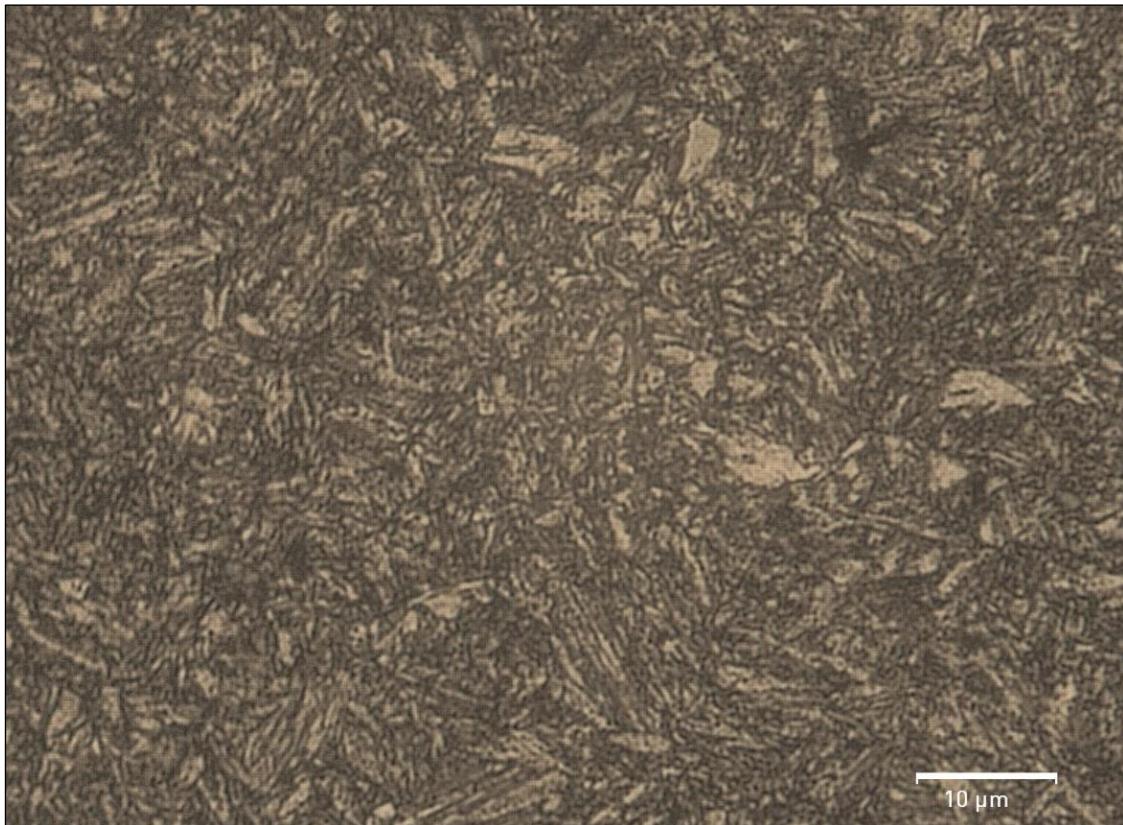


Fig. 1 Micrograph of steel specimens

Crack propagation tests were carried out under laboratory conditions ($23\pm 2^\circ\text{C}$ and $50\pm 5\%$ RH) per ASTM E647. Specimens were cyclically loaded by exciting sinusoidal wave form under 80 Hz test frequency on RUMUL cracktronic test system with stress ratio R of 0.1.

Results

Compliance Method

Crack length measurement can be done by different methods such as compliance, potential drop, laser interferometry and ultrasonic isoscanning. Among them, compliance technique is considered the most common method for estimating crack length. Compliance method is eligible for isotropic materials such as metals that exhibit linear elastic behavior by handling load and displacement data to determine crack propagation. The basic idea behind this method is based on the concept that stiffness decreases with increasing crack length on the specimen. Therefore, calibration curve correlates relationship between crack length and compliance. Compliance method is evaluated for a limited range in terms of normalized crack size. It is also attributed as elastic compliance of specimen because of introducing unloading part of elastic-plastic range, and it is a function of crack length. Therefore, compliance value changes by alternating crack length, which is inversely proportional to specimen size.

Closure phenomenon in fatigue cracks is based on continuously closing from crack tip, resulting in plasticity induced crack closure that alters compliance consistently on load-displacement curve. Friction of contact surfaces and plastic deformation result in hysteresis on the compliance curve that makes determination of opening stress more cumbersome. By introducing ΔK_{eff} (effective stress intensity factor) rather than using K (stress intensity factor) and R (stress ratio) together, stress ratio effect on fatigue crack growth can be significantly eliminated. As is known, plasticity induced crack closure is the responsible mechanism for varying crack growth rates under different stress ratios. It was observed that crack opening moment leads to change in compliance measurements. Compliance method is useful to monitor crack length of structures under alternating loading. It gives reasonable opening stress value from load-displacement curve in the range of 0.3 to 0.65 times specimen width in terms of crack length. Opening stress can also be estimated by following equation for constant amplitude loading conditions [22]:

$$\frac{S_0}{S_{max}} = A_0 + A_1 * R + A_2 * R^2 + A_3 * R^3 \quad \text{for } R \geq 0 \quad (1)$$

$$\frac{S_0}{S_{max}} = A_0 + A_1 * R \quad \text{for } -1 \leq R < 0 \quad (2)$$

$$A_0 = (0.825 - 0.34 * a + 0.05 * a^2) [\cos (\pi * S_{max} / 2\sigma_0)]^{1/a} \quad (3)$$

$$A_1 = (0.415 - 0.071 * a) * (S_{max} / \sigma_0) \quad (4)$$

$$A_2 = 1 - A_0 - A_1 - A_3 \quad (5)$$

$$A_3 = 2A_0 + A_1 - 1 \quad (6)$$

where σ_0 is the flow stress, S_0 is opening stress, S_{max} is maximum applied stress, R is stress ratio, a is constraint factor and A_0, A_1, A_2 and A_3 are the coefficients.

A constraint factor needs to be defined to discover stress state ahead of crack tip. Corresponding factor equals to 1 for plain stress conditions and 3 for plain strain conditions. Crack growth tests around near threshold were conducted under plain strain conditions in a controlled environment; therefore, later one was adopted for crack opening stress evaluation.

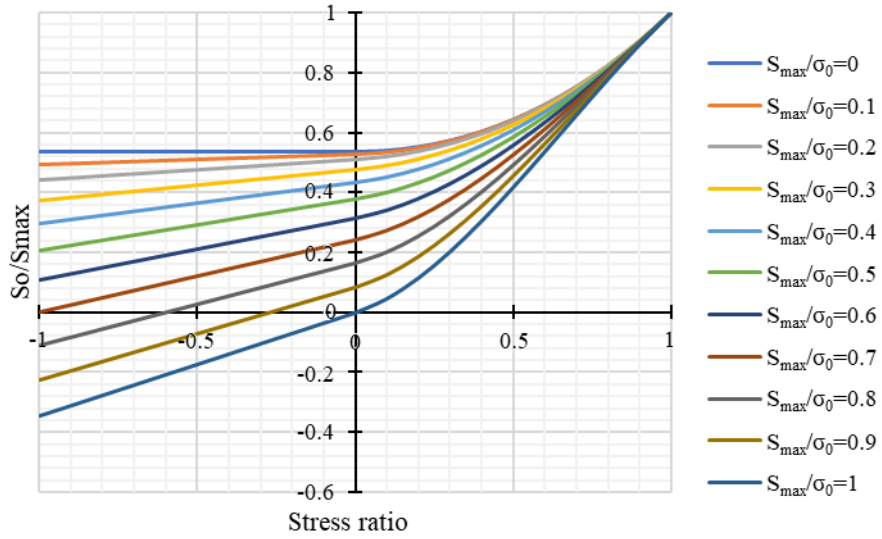


Fig. 2 Variation of normalized crack opening stress with stress ratio for constraint factor equals to 1

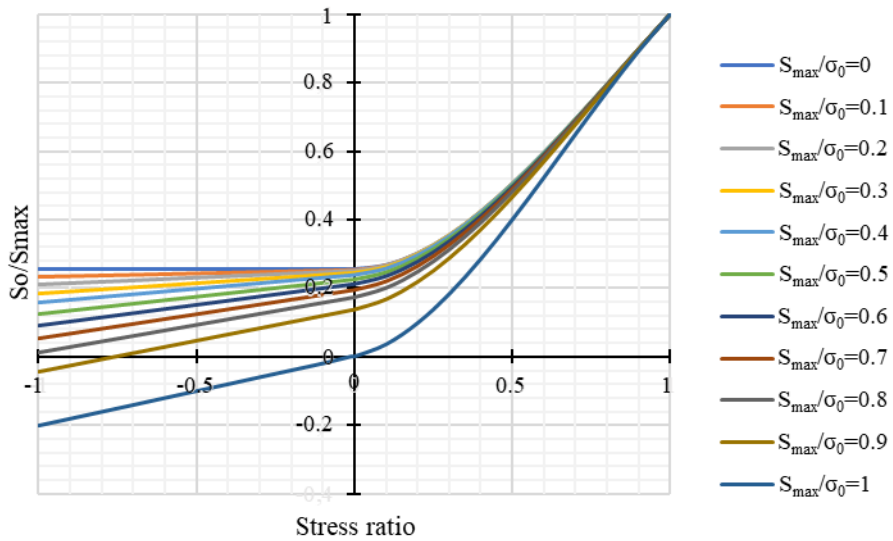


Fig. 3 Variation of normalized crack opening stress with stress ratio for constraint factor equals to 3

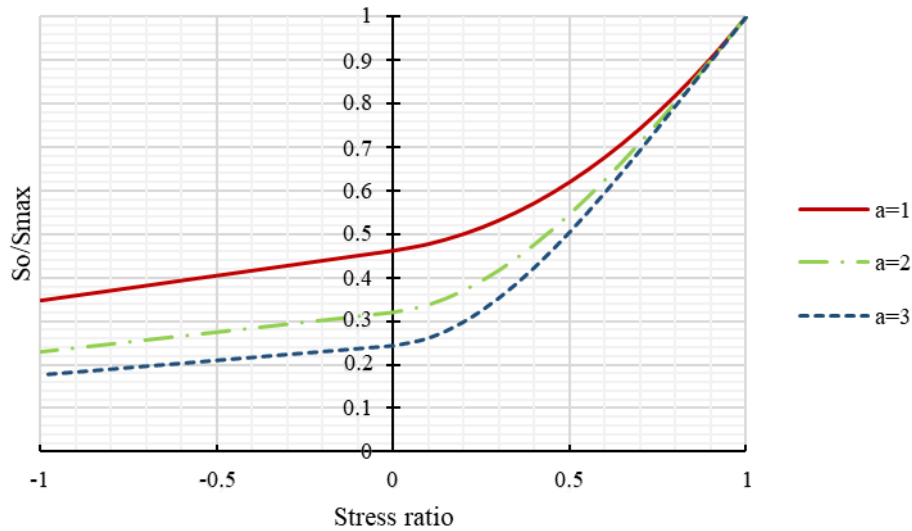


Fig. 4 Variation of normalized crack opening stress with stress ratio in case of $S_{max}/\sigma_0=1/3$

As seen from the graph, normalized crack opening stress exhibits lower value with increasing constraint factor, regardless of stress ratio.

Determining compliance by elastic unloading method is proposed by Clarke [23] in order to determine crack length and plastic work fragment ahead of crack tip. Compliance is also called as inverse stiffness function of crack length. Therefore, the relation between crack length and compliance is written in the form of following formulation:

$$EBC = f\left(\frac{a}{w}\right) \tag{7}$$

where E is elastic modulus of material, B is thickness, C is compliance, w is width and a is crack size.

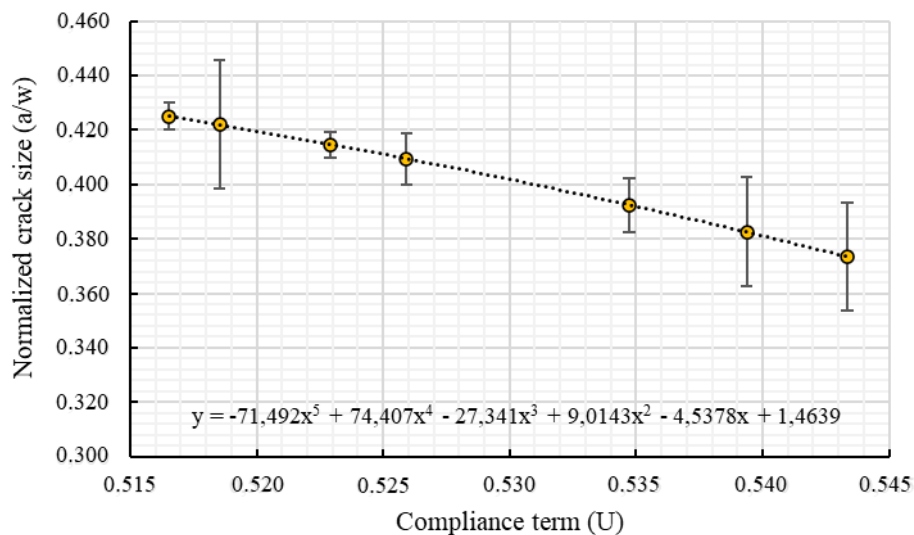


Fig. 5 Determination of crack size by compliance

For specimens with shallow cracks the following equations can be applied if the normalized crack size (a/w) is between 0.05 and 0.45 for SEB specimens [24]. This correlation is performed by least square polynomial regression.

$$\frac{a}{w} = 1.01878 - 4.5367 * u + 9.0101 * u^2 - 27.333 * u^3 + 74.4 * u^4 - 71.489 * u^5 \quad (8)$$

$$u = \frac{1}{\sqrt{\frac{BWCE}{S/4} + 1}} \quad (9)$$

where u is dimensionless compliance, S is span length of specimen.

During tests, crack sizes were measured at certain intervals and its correlation with compliance term was examined as shown in Fig. 5.

Compliance measurements were performed on unloading specimen to prevent possible errors because of inelastic strains while calculating slope of displacement versus load data. Compliance is also defined as inverse stiffness of material, and corresponding data contains nonlinearity at maximum and minimum values. Therefore, 10% of upper and lower part was omitted to prevent nonlinear effects and slope was determined via the least square regression fits on unloading part of curve. The accepted approach is to apply the fifth order polynomial fit proposed by Hudak and Saxena [25]. Even though compliance change may not be observed at high stress intensity factors because of stabilized crack, compliance variation can be observed at lower stress intensity factor, especially near thresholds.

To obtain accurate compliance value, 100 data pairs sampling rate is needed per each cycle. Among them, unloading part that is 50 data pairs is used to estimate opening stress. To determine opening stress, fully open crack slope value is firstly determined by help of least square. ASTM method uses the least square fit on the upper part of load-displacement curve which is in the range of about 25% to determine compliance value as shown in Fig. 6.

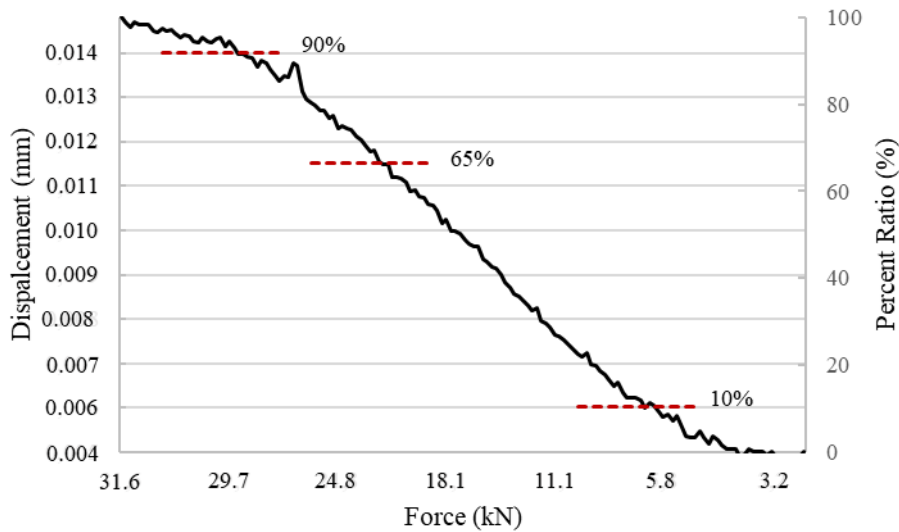


Fig. 6 Load-displacement curve

Compliance offset method was used to determine opening stress by introducing loading segment and overlapping range. In this study, loading segment was defined as 10% sliding on fully open part and overlapping range between each segment was 5% and variation from this slope gives opening stress by introducing specific deviation on slope value. This deviation can vary with sampling rate, therefore a larger sampling rate gives more reliable results.

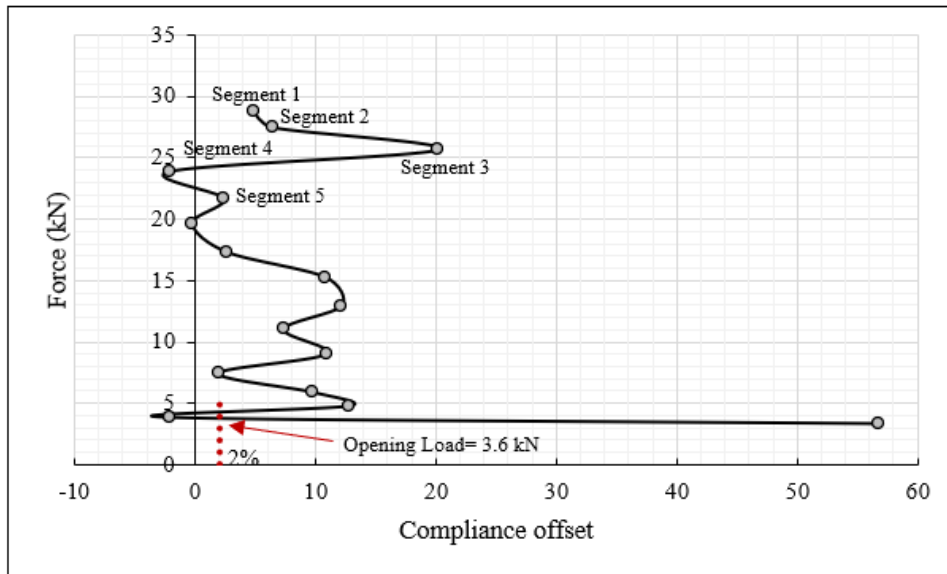


Fig. 7 Compliance offset method

High variability in compliance offset data resulted because of scattering in the data; nevertheless, the opening load can be estimated at 3.6 kN per ASTM assumption of 2% deviation given on Fig. 7.

Even though compliance change may not be observed at high stress intensity factors because of stabilized crack, compliance variation can be observed at lower stress intensity factor especially near thresholds. Compliance measurements were done throughout threshold tests and variation of crack size with compliance is shown in Fig. 8.

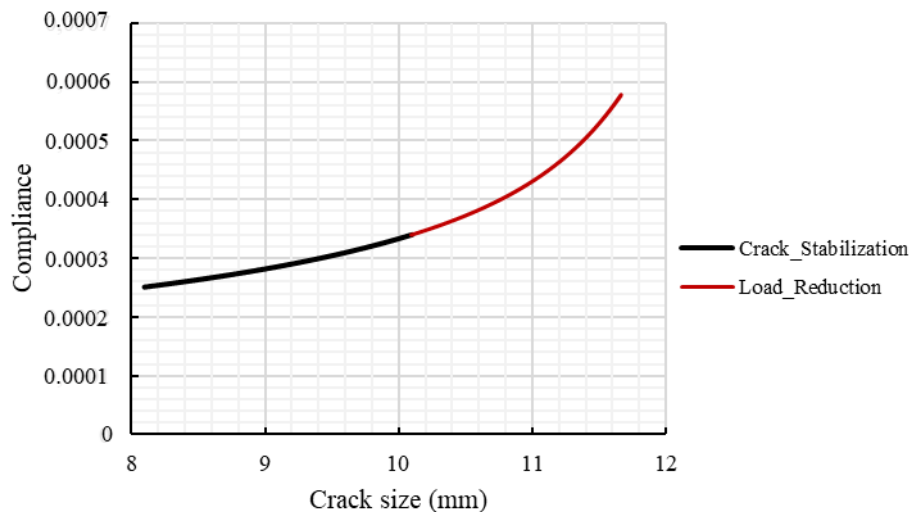


Fig. 8 Compliance change during each phase of test

Compression Precracking

Compression precracking is a method to obtain fatigue crack growth data with minimal load history effects. Possible reason for inaccurate threshold value is majorly load history effects arising from test procedure, specimen size and test configuration. In case of higher applied precracking loading, remote closure takes place and reduces driving force and results in higher threshold value. The advantage of compression precracking is that stress intensity is below zero while crack closing on pre-cracking period, therefore crack will directly open and not affected

by load histories under constant amplitude fatigue growth test. During compression precracking, monotonic compressive zone forms after first loading case and tensile yielding ahead of notch takes place after unloading and tensile plastic zone forms inside the compressive zone. As loading continues through testing, a cyclic plastic zone forms that results in small scale yielding and crack propagation. After crack keeps propagation, residual stress will relax and cyclic plastic zone size diminishes. It continues up to monotonic compressive zone size, then crack is arrested because of decreased driving force for crack growth. Advantageous of compression precracking is to provide fully open crack which eliminates possible crack closure effects, therefore it results in less crack propagation rates at low stress intensities. Crack growth rate around near threshold depends on increased stress intensity due to crack growth and ascending threshold because of arising crack closure effects. After certain length propagation near threshold value, crack closure builds up becomes slower and increase of stress intensity gets dominant for crack extension.

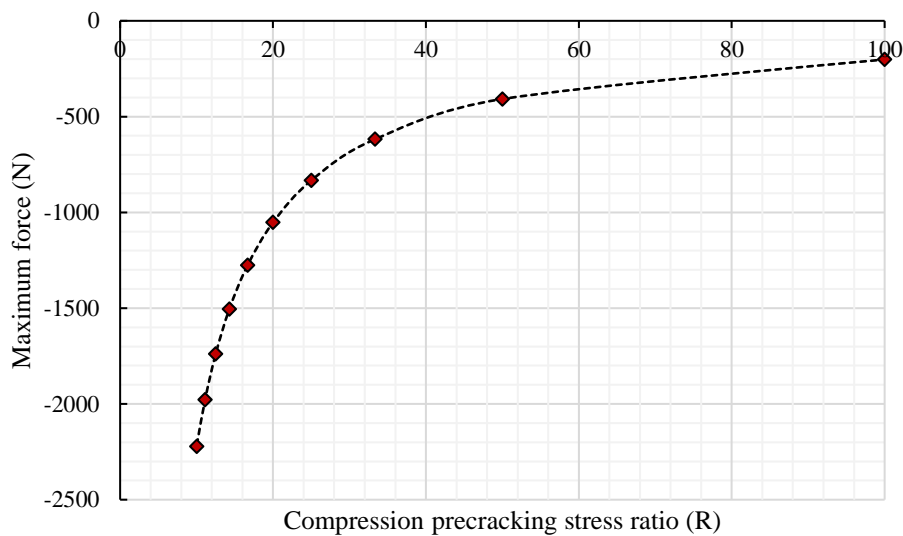


Fig. 9 Variation of maximum precrack force with stress ratio

Before compression, precracking; stress concentration around crack tip was done via razor blade operation. Razor blade is accepted as beneficial method for forming sharp crack around 20 μm because of little plastic deformation for precracking. After EDM notch preparation, the notch is sharpened by razor blade with 1 μm diamond paste. EDM notch is machined by 30 μm in diameter wires for precise dimensions. Precracking tests were carried out under constant amplitude compressive loading that enables tensile yield ahead of crack tip, and this tensile zone is responsible for straight and natural crack. By extension of fatigue crack, tensile cyclic plastic zone decreases because of relaxation of internal stresses and crack arrests after reaching on monotonic compressive zone. Amount of crack growth for precracking can be correlated with compressive plastic zone size. Arrested crack is called as non-propagating crack under compressive loading because of not available driving force. Compressive precracking tests were performed at stress ratio: $R=10$, $R=20$ and $R=40$ via four point bending setup on RUMUL resonant fatigue test system by keeping constant ΔK for each case. Test loads were determined based on Irwin plastic zone assumption. Lower and upper roller distance was 24 mm for each case, and oscillatory load was calculated as 20 kN for compression precracking tests. By increasing stress ratio, maximum force converges to zero as shown in Fig. 9 and minimum force converges to -20 kN in case of predetermined 10 kN amplitude loading condition. In other words, fatigue crack threshold values for compression precracked specimens with higher stress ratio converges to proximate threshold values after certain load ratio.

Therefore, R of 40 for compression precracking was chosen as the highest stress ratio, since the threshold values for higher stress ratios will resemble to each other.

To identify the effect of compression precracking on near threshold regime, three specimens were tested under different stress ratios as shown in Fig. 10 and one of the specimens not precracked for comparison. Compression precracking loading is estimated based on an Irwin tip radius of 0.25 mm over plain stress condition. Under subsequent cyclic loading, cyclic plastic zone size decreases because of relation of residual stresses and this results in decreasing driving force for crack propagation and crack arrets around monotonic compressive zone.

$$r_p, \text{ Plain Stress} = \left(\frac{1}{2\pi}\right) \left(\frac{K_{max}}{\sigma_y}\right)^2 \quad (10)$$

where r_p is Irwin radius, K_{max} is maximum stress intensity factor and σ_y is yield strength of material. K_{max} can be calculated by given equations below;

$$K_{max} = \left(\frac{Y * M_{max}}{B * \sqrt{(W)^3}}\right) \quad (11)$$

$$Y_{SEB} = 6 * \left(\frac{\sqrt{(2 * \tan(\frac{a}{W}))}}{\cos(\frac{a}{W})}\right) * (0,923 + 0,199 * \left(1 - \sin\left(\frac{a}{W}\right)\right)^4) \quad (12)$$

where M_{max} is maximum moment, B and W are thickness and width of specimens respectively, Y is geometry factor, a is crack size of specimen including notch length.

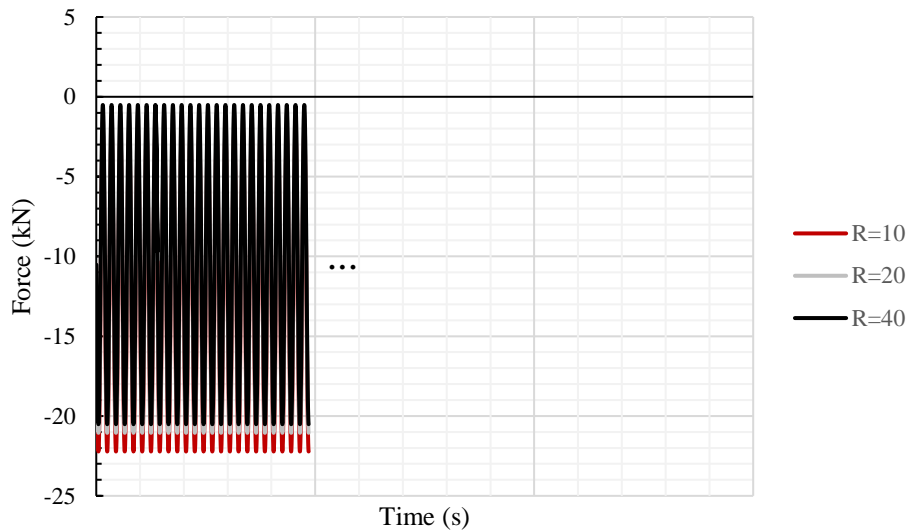


Fig. 10 Load profile of compression precracking for different stress ratios

Tests were continued until 2E+06 cycles, then non-propagating crack was measured through optical microscope for each specimen as shown in Fig. 11. After compression precracking, non-propagating crack needs to advance at least three monotonic compressive zone sizes to reach steady state crack growth conditions. Non-propagating crack size was around 0.2 mm or less, and it is known that precracking size is less than cyclic tensile zone consisting of after unloading. In order to generate reliable fatigue crack growth data, precracking size needs to be outside monotonic compressive zone by ensuring small scale yielding ahead of crack tip. This is achieved by tensile fatigue loading after compression precracking in order to be free in terms of residual stresses.

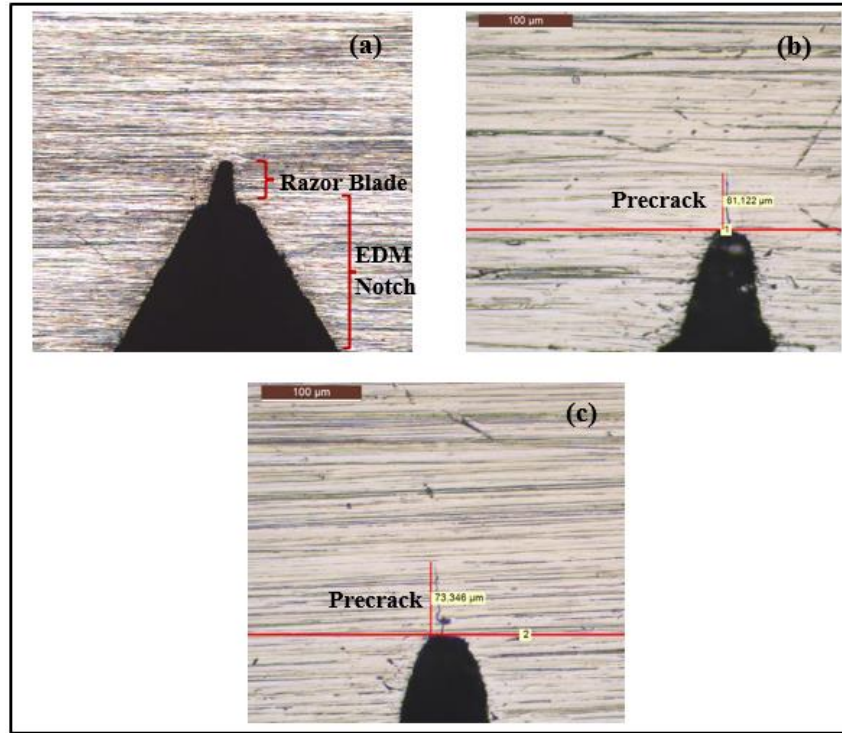


Fig. 11 Non-propagating crack after compression precracking:
a) Razor blade application before precracking; b) Front side micrograph;
c) Back side after formation of non-propagating crack

Constant amplitude loading is performed just below the threshold value until increased crack propagation rate slightly. In this point, most annoying part is to estimate initial ΔK value, since initial data is affected by tensile residual stresses form precracking. Tests were initiated at small stress intensities to propagate crack. After $5E+05$ cycles, load increment was increased as 10% in case of not observed crack propagation. This sequence is continued until crack propagation having stabilized rate. Crack size having at least two- or three-times plastic zone size enables to reach steady state crack growth rate under constant amplitude loading after providing 1-1.5 mm crack advancement. During propagation phase, crack plane is yielded and formed residual stresses affects propagation of crack beyond plastic zone. Crack arrest is caused by residual stresses and loading below threshold stress. Therefore, residual stress effects are eliminated for following constant amplitude testing in case of pre-crack size is around plastic zone size. In this study, ΔK initial was chosen as $4.5 \text{ MPa}\sqrt{\text{m}}$ for R of 0.1. Then, a minimum of 1.5 mm of crack propagation was allowed to ensure that the crack was stabilized.

Load reduction method was followed after crack stabilization to find out precise threshold value around $1E-10$ crack growth rate. At least five data points were observed that test was stopped by assuming crack not propagating around near threshold region because of dominant closure effects on crack growth rate.

NASGRO crack growth approach was used to estimate ΔK_{th} while post-processing of the data analysis [26]. Expression is given by following equation;

$$\frac{da}{dN} = C \left(\frac{(1-f)}{(1-R)} \Delta K \right)^n \frac{\left(1 - \frac{\Delta K_{th}}{\Delta K} \right)^p}{\left(1 - \frac{K_{max}}{K_c} \right)^q} \quad (13)$$

where crack growth rate (da/dN) depends on following parameters: C and n are constants, f is Newman's crack opening function, p and q are responsible for slope change in threshold and unstable crack growth region respectively, ΔK is stress intensity factor range, ΔK_{th} is threshold

stress intensity factor range, K_{max} is maximum applied stress intensity factor, K_c is critical stress intensity factor and R is stress ratio.

Newton's crack opening function (f) can be calculated by following formula [21];

$$f = \frac{K_{opening}}{K_{maximum}} = \begin{cases} \max R \text{ or } (A_0 + A_1 * R + A_2 * R^2 + A_3 * R^3) & R \geq 0 \\ A_0 + A_1 * R & R < 0 \end{cases} \quad (14)$$

where $K_{opening}$ is opening stress intensity factor and $K_{maximum}$ is maximum stress intensity factor.

The equation fits fatigue crack growth data using the logarithmic square method by minimizing errors. The material constants C and n were taken as the fitting parameters and the parameter q was set to zero because of only interested in near threshold region [27].

The following NASGRO equations can be used to evaluate the threshold change as a function of the stress ratio [28]. C_{th}^p , C_{th}^m and ΔK_1 are materials constants, they are estimated by least square fitting with fatigue threshold (ΔK_{th}) data. ΔK_1 is the stress intensity threshold range as the stress ratio approaches to 1. ΔK_1^* takes into account small crack parameter that is called as a_0 [29].

$$\Delta K_{th} = \Delta K_1^* * \left[\frac{\left(\frac{1-R}{1-f}\right)^{(1+RC_{th}^p)}}{(1-A_0)^{(1-R)(C_{th}^p)}} \right] \quad R \geq 0 \quad (16)$$

$$\Delta K_{th} = \Delta K_1^* * \left[\frac{\left(\frac{1-R}{1-f}\right)^{(1+RC_{th}^m)}}{(1-A_0)^{(C_{th}^p - RC_{th}^m)}} \right] \quad R \geq 0 \quad (17)$$

$$\Delta K_1^* = \Delta K_1 * \sqrt{\frac{a}{(a+a_0)}} \quad (18)$$

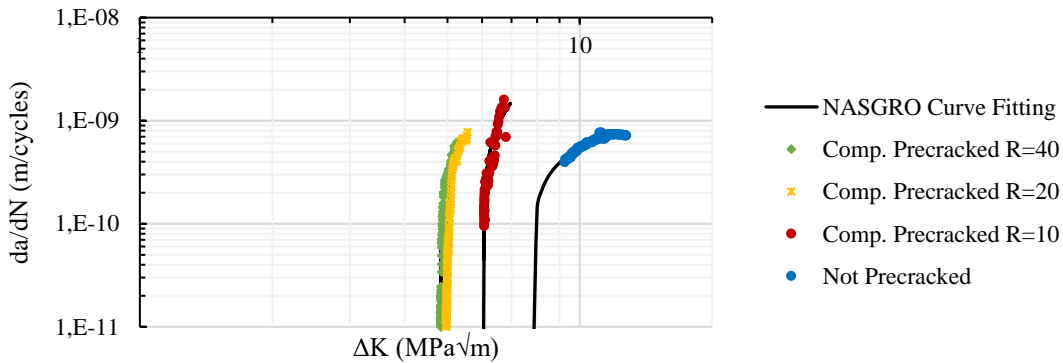


Fig. 12 NASGRO curve fitting after crack growth tests

Curve fitting by least square method helps to estimate stress intensity threshold range. As a result, the resultant curves were plotted only on near threshold data by applying NASGRO curve fit as shown in Fig. 12. For not precracked specimen; initial ΔK was started with 5 MPa√m and at least 2E+06 cycles loaded to observe fatigue crack. Nevertheless, fatigue crack was not initiated on this stress level even though enough stress concentration formed through razor blade nevertheless it was not sufficient to initiate crack ahead of the notch then ΔK was increased as %10 of predefined initial ΔK value. This procedure was continued until ΔK was equal to 15 MPa√m. Then, natural crack was formed on notch region and stabilized after 1.5 mm advancement. During load reduction, crack propagated fast because of high stress level and crack length reached its limit because of specimen geometry. Therefore, crack growth data

points were not recorded around 10^{-10} m/cycles. Nevertheless, NASGRO curve fitting enables to estimate long crack threshold value after least square for not precracked specimen test. Accordingly, long crack threshold values were found 4.82, 4.96, 6.06 and 7.97 MPa \sqrt{m} for R of 40, 20, 10 and not precracked specimens respectively.

Long crack threshold values for each case were determined and the effect of compression-compression precracking was evaluated. Accordingly, R of 40 was resulted as lowest threshold value that means more accurate estimate on threshold value can be done through that stress ratio as design criteria. Indeed, lower stress ratio for compression precracking resulted in remote closure taking place and reducing driving force, hence higher threshold value was obtained. It is suggested that higher stress ratio for compression precracking can be chosen for accurate and reliable fatigue threshold value. If compression precracking was not performed before starting crack growth tests, it was resulted as higher threshold as expected because of load history effects.

Discussion

The accuracy of compliance measurements provides correlation about assessment of crack closure responsible for stress ratio effect on fatigue crack growth rate, which introduces effective stress intensity factor. In small crack lengths, the compliance value increases with the increase of the load, while the compliance starts to diverge at larger crack lengths. Determining of opening stress through compliance method is difficult and confusing because of hysteresis and measurement noise on data. Compliance variation is caused by change in crack size that alters contacted region and change in plastic zone size. It is generally accepted that usage of 2% deviation from compliance offset gives sensible results. Crack opening stress through compliance method can be attributed more than 3% deviation on load displacement curve. Opening stress can be estimated by assuming an offset of 1.5% on the load-displacement curve. In case total variation of load displacement curve is very small; in other words, where the slope change is not easily seen, opening stress determining can be problematic and brings large scatter on results. For such cases, ASTM compliance offset through 2% deviation leads to evaluating less opening stress value compared to larger variation of compliance instances having distinct slope change. Preference of larger deviation such as 10% on compliance offset value results in less scatter on data but shifting effective stress intensity curve to larger values. Among other methods, ASTM is admitted as compliance offset method. Nevertheless, the downside of the method is that poor precision leads to large scatter on compliance measurements. Another disadvantage is that ASTM offset method may alter with variation of stress ratio.

Compression precracking before crack growth tests causes faster crack growth rates compared to load reduction procedure and resulted as lower threshold value. Threshold values are affected by initial ΔK under load reduction scenario. On the other hand, cracks will be fully open after compression precracking and reaches steady state under constant amplitude loading. Therefore, providing stabilized crack before load reduction approaches crack growth to effective stress intensity and deviation around threshold is minimized. Because of difficulties like to control crack growth and keep a sufficient crack length under tensile-tensile precracking; compression precracking is more preferable. Precracking productivity depends on grain boundary orientation in terms of aligned and elongated grains. It is desired to apply small ΔK for precracking to minimize tensile residual stresses. After precracking, small scale yielding ahead of crack tip front takes place under cyclic compression. Non-propagating crack size is around 0.2 mm or more, and it is known that precracking size is less than cyclic tensile zone consisting of after unloading. In order to generate reliable fatigue crack growth data, precracking size needs to be outside of monotonic compressive zone by ensuring small scale yielding ahead of crack tip. This is achieved by tensile fatigue loading after compression precracking in order to be free in terms of residual stresses.

Long cracks need to be fully opened on steady state region, then load reduction can be applied to obtain accurate threshold value by assuring fatigue crack growth tests performed with eliminated residual stresses. Even though compression precracking provides minimization of load history effects, crack propagation is desired to be sure on eliminated of closure effects. ASTM E647 load reduction procedure exhibits low crack propagation rate and high threshold values because of having roughness and oxide induced crack closure, which is responsible for observing rough crack flank. Precracking stress value shall be minimum as much as possible to decrease residual stress effects ahead of crack tip.

Crack growth takes place by fulfilled following condition: Applied loading is larger than $K_{max,th}$ and ΔK_{th} . Long crack threshold value is a material property and independent of crack size and specimen geometry. Small cracks advance on regions owning in-situ or pre-existing stress concentration that can be caused by slip bands, dislocation pile-up or existing defects. Cyclic deformation provides fatigue damage formation though dislocation pile-up, persistent slip band formation and accordingly presents available condition for initiation phase of crack. Short crack behavior can be summarized as their dependence on crack length, having higher crack growth rates, advancement even below long crack threshold value and variance of threshold with crack size.

Cracks may not be initiated at maximum allowable rates under load reduction for AISI 4340 steels; however, precracking enables initiation of cracks around ΔK_{th} by minimizing load history effects. Even though it is considered that compression precracking provides presenting more accurate fatigue crack growth data with minimal load history effects compared to traditional methods. After compression precracking, non-propagating crack needs to advance at least three monotonic compressive zone sizes to reach steady state crack growth conditions.

Crack closure is caused by tensile part of loading for long cracks under small scale yielding conditions. In small scale yielding, crack closure effect is caused by plasticity, roughness and oxide induced crack closure. Plasticity induced crack closure is not observed on plain strain conditions, since local wedge near crack tip takes place because of plastic shear deformation in wake of crack. Source of internal stresses is stress concentration regions such as notch, hole, microstructural defects etc. And internal stress asymptotically decreases by distance to move away. However, applied stress increases by increasing crack length and there exist competitions in terms of total stress. If applied stress is less than ΔK_{th} and K_{max} , crack is arrested since total stress is insufficient for propagation. Elimination of internal stress is attributed to fatigue crack growth behavior of long cracks. Local stress ratio will be higher at crack tip than remote load ratio because of existence of internal stresses.

Crack closure becomes stabilized by growing from small to long crack, and it increases by increasing crack length until steady state. In this region, closure in terms of crack wake plasticity is maximized then its effectiveness diminishes by increasing effective stress. Presence of crack closure enables to contact of crack flakes under unloading, then results in change in slope on compliance curve. By increasing stress ratio for long cracks, crack closure effects diminish and become R of 0.7 condition. Crack closure for small cracks slowly increases by increasing crack size, that means threshold stress for small cracks increases until certain value that small crack approaches to long cracks.

Conclusions

Threshold stress becomes significant especially for structures having high cycle loading and resulting in high percentage of initiation and short time for propagation, so life estimation is necessary with accurate threshold stress. Long crack threshold value is basically used in design value for damage tolerant structures, however it is known that small cracks exhibit different crack growth rates than long cracks. To clarify differences in propagation rate, crack closure

concept needs to be well grasped. The following conclusions drawn from this study are listed below:

- Compliance curve is restricted on $0.25 < a/w < 0.8$ region to represent appropriate calibration result.
- Steady state region on crack growth curve represents crack propagation with constant rate until plastic zone size with unchanged crack sharpness. Threshold value of a component is defined during design phase to estimate safe operation life during service therefore accurate data is significant for durability purposes.
- Residual life of a component is remarkably affected with altering threshold value. For instance, small change on threshold value results in considerable change in residual characteristics of a component.
- Higher stress ratios for compression precracking tests are advised for more accurate fatigue threshold value.
- Crack size after compression precracking is directly related with monotonic compressive zone after first compressive loading.
- Long crack threshold value exhibited high scatter which is around 20% for precracked specimens. By using polynomial fit to entire region; fatigue crack growth rate and threshold value can be estimated.
- The probable cause of the erroneous threshold value is largely due to load history effects from the test procedure, sample size, and test configuration. In case of higher applied precracking loading, remote closure takes place and reduces driving force and results in higher threshold value.

References

1. James M, Forth S, Newman J. Load history effects resulting from compression precracking. *Journal of ASTM International*. 2005;2(9): 12025.
2. Pippan R, Hohenwarter A. Fatigue crack closure: a review of the physical phenomena. *Fatigue & Fracture of Engineering Materials & Structures*. 2017;40(4): 471–495.
3. Li S, Zhang Y, Qi L, Kang Y. Effect of single tensile overload on fatigue crack growth behavior in DP780 dual phase steel. *International Journal of Fatigue*. 2018;106: 49–55.
4. Hubbard RP. Crack growth under cyclic compression. *Journal of Basic Engineering*. 1969;91(4): 625–630.
5. Pearson S. Initiation of fatigue cracks in commercial aluminium alloys and the subsequent propagation of very short cracks. *Engineering Fracture Mechanics*. 1975;7(2): 235–247.
6. Newman JC. A nonlinear fracture mechanics approach to the growth of small cracks. *AGARD Behaviour of Short Cracks in Airframe Components*. 1983. Available from: <https://ntrs.nasa.gov/citations/19830025829> (Accessed 24th Nov 2022).
7. Elber W. The significance of fatigue crack closure. In: *Damage Tolerance in Aircraft Structures*. 1971. p.230-242.
8. James M, Forth S, Johnston W, Newman JA, Everett R. Effects of compression precracking on subsequent crack growth. In: *15th European Conference of Fracture Advanced Fracture Mechanics for Life and Safety Assessments (ECF15)*. Stockholm, Sweden; 2013.
9. Maierhofer J, Pippan R, Gänser H-P. Modified NASGRO equation for short cracks and application to the fitness-for-purpose assessment of surface-treated components. *Procedia Materials Science*. 2014;3: 930–935.
10. Newman Jr. JC, Yamada Y. Compression precracking methods to generate near-threshold fatigue-crack-growth-rate data. *International Journal of Fatigue*. 2010;32(6): 879–885.

11. Chapetti MD. Estimation of the plain high-cycle fatigue propagation resistance in steels. *Materials Research*. 2002;5(2):101–105.
12. Suresh S, Ritchie RO. Propagation of short fatigue cracks. *International Metals Reviews*. 1984;29(1): 445–475.
13. McEvily AJ. The growth of short fatigue cracks: a review. *Transactions on Engineering Sciences*. 1970;13: 93–107.
14. Sadananda K, Nani Babu M, Vasudevan AK. A review of fatigue crack growth resistance in the short crack growth regime. *Materials Science and Engineering: A*. 2019;754: 674–701.
15. Tabernig B, Pippan R. Determination of the length dependence of the threshold for fatigue crack propagation. *Engineering Fracture Mechanics*. 2002;69(8): 899–907.
16. Meggiolaro M, Miranda A, Decastro J. Short crack threshold estimates to predict notch sensitivity factors in fatigue. *International Journal of Fatigue*. 2007;29(9-11): 2022–2031.
17. Sadananda K, Vasudevan AK. Short crack growth and internal stresses. *International Journal of Fatigue*. 1997;19(93): 99–108.
18. Lawson L. Near-threshold fatigue: a review. *International Journal of Fatigue*. 1999;21: 15–34.
19. Grasso M, De IA, Xu Y, Haritos G, Mohin M, Chen YK. Corrigendum to “An Analytical Model for the Identification of the Threshold of Stress Intensity Factor Range for Crack Growth”. *Advances in Materials Science and Engineering*. 2018;2018: 1–2.
20. *Heat Treatment of Carbon and Low-Alloy Steel Parts Minimum Tensile Strength Below 220 ksi (1517 MPa)*, AMS 2759-1D, 2007. Available from: <https://www.sae.org/standards/content/ams2759/1d/>
21. *Standard Test Method for Measurement of Fatigue Crack Growth Rates, ASTM E647-15e1, December 2016*. Available from: www.astm.org
22. Newman JC. A crack opening stress equation for fatigue crack growth. *International Journal of Fracture*. 1984;24(4): R131–R135.
23. Clarke GA, Andrews WR, Paris PC, Schmidt DW. Single Specimen Tests for JIc Determination. Mechanics of Crack Growth, ASTM STP 590. In: *American Society for Testing and Materials*. Philadelphia; 1976. p.27-42.
24. *Standard Test Method for Measurement of Fracture Toughness, ASTM E1820-11E2, 2011*. Available from: www.astm.org
25. Saxena A, Hudak SJ. Review and extension of compliance information for common crack growth specimens. *International Journal of Fracture*. 1978;14(5): 453–468.
26. Forman RG, Shivakumar V, Cardinal JW, Williams LC, McKeighan PC. *Fatigue crack growth database for damage tolerance analysis*. National Technical Information Service, Springfield, Virginia, USA. Technical Report number: PB2005-110675, 2005.
27. Patriarca L, Filippini M, Beretta S. Short-crack thresholds and propagation in an AISI 4340 steel under the effect of SP residual stresses. *Fatigue & Fracture of Engineering Materials & Structures*. 2018;41(6): 1275–1290.
28. *NASGRO, N. J. S. C. Fatigue Crack Growth Computer Program Nasgro Version 4.2–Reference Manual*. 2006.
29. El Haddad MH, Topper TH, Smith KN. Prediction of non propagating cracks. *Engineering Fracture Mechanics*. 1979;11(3): 573–584.

THE AUTHORS

Caliskan S. 
e-mail: caliskan.salim@metu.edu.tr

Gurbuz R. 
e-mail: rgurbuz@metu.edu.tr